



PCCP

**Evidence for  $\pi_{\text{CHR}} \rightarrow d_{\text{M}}$  Bonding in Transition Metal Carbene Compounds ( $L_nM=CHR$ ) and Its Decisive Role in the  $\alpha$ -Agostic Effect**

Journal:	<i>Physical Chemistry Chemical Physics</i>
Manuscript ID	CP-ART-08-2022-003870
Article Type:	Paper
Date Submitted by the Author:	22-Aug-2022
Complete List of Authors:	Lin, Xuhui; Southwest Jiaotong University, School of Life Science and Engineering Tian, Weiqin; Southwest Jiaotong University Wu, Wei; Xiamen University, Mo, Yirong; University of North Carolina at Greensboro, Naniscience

SCHOLARONE™  
Manuscripts

## ARTICLE

# Evidence for $\pi_{\text{CHR}} \rightarrow d_{\text{M}}$ Bonding in Transition Metal Carbene Compounds ( $L_n\text{M}=\text{CHR}$ ) and Its Decisive Role in the $\alpha$ -Agostic Effect

Xuhui Lin<sup>a,\*</sup>, Weiqin Tian<sup>a</sup>, Wei Wu<sup>b,\*</sup>, Yirong Mo<sup>c,\*</sup>

Received 00th January 20xx,  
Accepted 00th January 20xx

DOI: 10.1039/x0xx00000x

It has been generally recognized that the  $\alpha$ -agostic interaction ( $\text{M}\cdots\text{H}\cdots\text{C}$ ) in transition metal carbene compounds  $L_n\text{M}=\text{CHR}$  ( $\text{R}=\text{H}$ ,  $\text{Me}$  etc.) can be interpreted with a double metal-carbon bonding model. This bonding model involves the reorganization of the  $\sigma$  component, which can be illustrated in terms of three-center two-electron (3c-2e)  $\text{M}\cdots\text{H}\cdots\text{C}$  covalent bond as in transition metal alkyl compounds. Herein, we propose an alternative partial triple metal-carbon bonding model to elucidate the agostic interaction in  $L_n\text{M}=\text{CHR}$ . Apart from the well-defined  $\sigma$  and  $\pi$  bonds, there exists a seemingly weak but decisive third force, namely the  $\pi_{\text{CHR}} \rightarrow d_{\text{M}}$  bonding between an occupied  $\pi$ -like symmetric CHR orbital and a vacant metal  $d$  orbital, which is the true origin of the  $\alpha$ -agostic effect. This partial triple bonding model is authenticated on both Fischer- and Schrock-type carbenes by an ab initio valence bond (VB) method or the block-localized wavefunction (BLW) method, which has the capability to quantify this notable  $\pi$  bonding and further demonstrate its geometric, energetic and spectral impacts on agostic transition metal carbene compounds. We also show that ancillary ligands can modulate the  $\pi_{\text{CHR}} \rightarrow d_{\text{M}}$  bonding through electronic and steric effects.

## Introduction

Transition metal (TM) carbene compounds have been fascinating chemists, as they are key reactants, intermediates and transition states in various catalytic processes.<sup>1-5</sup> Since the first TM carbene compound was synthesised in 1964 by Fischer,<sup>6</sup> there have been an array of such compounds discovered and an intense assessment has been prompted to understand their structural and functional peculiarities, particularly the nature of metal-carbon bonds therein.<sup>7,8</sup> So far a double bonding model involving both  $\sigma$  and  $\pi$  interactions has been well envisioned, though certain computational and experimental evidences demonstrate that the metal-carbon bond orders are generally less than or equal to unity.<sup>9</sup> Besides the expected short double  $\text{M}=\text{C}$  bond distances, several TM carbene compounds ( $L_n\text{M}=\text{CHR}$ ) also display acute  $\text{M}-\text{C}-\text{H}$  angles (less than  $120^\circ$ ) yet large  $\text{M}-\text{C}-\text{R}$  angles (up to  $150\sim 170^\circ$ ), low  $\text{C}-\text{H}$  bond stretching frequencies and upfield carbon chemical shifts.<sup>10</sup>

In 1980, Goddard et al. proposed the hypothesis of carbene pivoting and subsequently traced this unusual structural

deformation to the “intramolecular interaction between carbene lone pair and corresponding metal acceptor orbital” (i.e. the  $\sigma$  bond, as seen in Fig. 1(a)).<sup>11</sup> Specifically, the carbene lone pair can interact with the metal’s  $d_{z^2}$  orbital and form a dative  $\sigma$  bond. However, if the carbene is tilted, the lone pair can interact with the  $d_{xz}$  orbital as well. The latter interaction is responsible for the acute  $\text{M}-\text{C}-\text{H}$  angle. Goddard et al. also pointed out that there is a weak  $\pi_{\text{CHR}} \rightarrow d_{\text{M}}$  bonding interaction (Figure 1b), though they believed it to be marginal and not responsible for the agostic structures in TM carbenes. For the agostic interaction in TM alkyl compounds similarly with acute  $\text{M}-\text{C}-\text{H}$  angles, however, a three-center two-electron (3c-2e) covalent bond between an occupied  $\text{C}-\text{H}$  orbital and a vacant  $d$  orbital of metal centre ( $\sigma_{\text{CH}} \rightarrow d_{\text{M}}$ ) was proposed by Green and Brookhart,<sup>12-14</sup> but its general applicability has been questioned<sup>15</sup>. Recently, this 3c-2e  $\sigma_{\text{CH}} \rightarrow d_{\text{M}}$  was described as a  $\pi$ -bond character bonding of TM alkyl compounds by Copéret and co-workers,<sup>16</sup> which has been quantified by ab initio valence bond theory<sup>17</sup>. In this work, we adopt the original concept of  $\pi_{\text{CHR}} \rightarrow d_{\text{M}}$  bonding to describe the agostic interaction.

In consistent with Goddard et al.’s bonding model, Eisenstein and Jean also attributed the  $\alpha$ -agostic interaction in TM alkyl compounds to the reorganization of the  $\sigma_{\text{M}-\text{C}}$  bond,<sup>18</sup> while the negative hyperconjugation from  $\text{M}-\text{C}$  bond to the whole alkyl group should be responsible for the formation of the  $\beta$ -agostic interaction<sup>19</sup>. Alternatively, Lu et al. argued that the formation of  $\beta$ -agostic structures is driven by the short London dispersion effect.<sup>20</sup>

<sup>a</sup> School of Life Science and Engineering, Southwest Jiaotong University, Chengdu, Sichuan 610031, China. E-mail: [xuhui.lin@swjtu.edu.cn](mailto:xuhui.lin@swjtu.edu.cn)

<sup>b</sup> Address here. The State Key Laboratory of Physical Chemistry of Solid Surfaces, iChEM, Fujian Provincial Key Laboratory of Theoretical and Computational Chemistry and College of Chemistry and Chemical Engineering, Xiamen University, Xiamen, Fujian 361005, China. E-mail: [weiwu@xmu.edu.cn](mailto:weiwu@xmu.edu.cn)

<sup>c</sup> Department of Nanoscience, Joint School of Nanoscience and Nanoengineering, University of North Carolina at Greensboro, Greensboro, NC 27401, United States. E-mail: [y\\_mo3@uncg.edu](mailto:y_mo3@uncg.edu) (YM)

Electronic Supplementary Information (ESI) available: [details of any supplementary information available should be included here]. See DOI: 10.1039/x0xx00000x

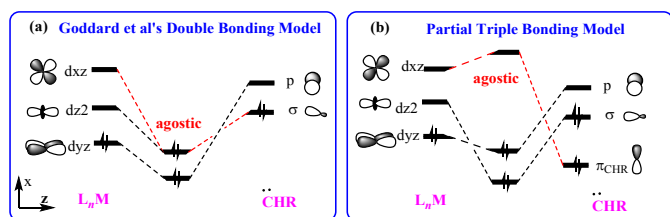


**Figure 1.** Bonding model for  $\alpha$ -agostic interaction in transition metal carbene compounds.

Despite the controversies over the nature of agostic interactions in TM alkyl compounds,<sup>21, 22</sup> there have been few different proposals from the Goddard et al.'s for the nature of the  $\alpha$ -agostic interaction in TM carbene compounds. In this work, however, we propose an alternative partial triple bonding model to elucidate the agostic TM carbenes, in which the  $\pi_{\text{CHR}} \rightarrow d_{\text{M}}$  interaction between an occupied  $\pi$ -like symmetric CHR orbital and a vacant d orbital is the driving force for the  $\alpha$ -agostic interaction (Fig. 1(b)). The focus in this study is thus on the precise role of the metal's orbital  $d_{xz}$  which interacts with the  $\pi_{\text{CHR}}$  orbital or the distortive  $\sigma$  lone pair in agostic TM carbenes. To evaluate and quantify such  $\pi_{\text{CHR}} \rightarrow d_{\text{M}}$  interactions, we resorted to the ab initio valence bond (VB) theory which provides a workable solution as it constructs wave functions for Lewis (resonance or electron-localized) structures with strictly localized atomic or fragmental orbitals.<sup>23-26</sup> In particular, the block-localized wavefunction (BLW) method, which incorporates the advantages of both MO and VB theories, is able to explore the geometric, energetic and spectra impacts of delocalization (and thus the  $\pi$  interaction) on transition metal carbene compounds.<sup>27-29</sup> Fig. 2 shows the computational models in this work.

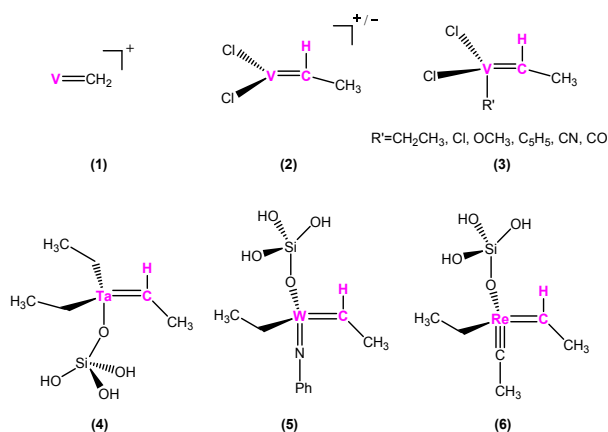


**Figure 2.** Computational models of experimental TM carbene compounds with agostic interactions.

## Results and Discussion

The first case discussed here is the ligand-free model system  $[\text{V}=\text{CH}_2]^+$ , whose geometries were optimized at the PBE0-D3(BJ)/Stuttgart (6-311G\*\*) level. Our computational results show that the  $C_s$  structure is more stable than the  $C_{2v}$  structure by 1.5 kcal/mol, which is consistent with the literature.<sup>30</sup> In

contrast to a usual metal alkylidene structure of  $C_{2v}$  symmetry, the global minimum  $C_s$  structure exhibits significant structural deformation, including an acute  $\text{V}-\text{C}-\text{H}'$  angle ( $80.7^\circ$ ), a large  $\text{V}-\text{C}-\text{H}$  angle ( $163.9^\circ$ ) and a stretched  $\text{C}-\text{H}'$  bond ( $1.145\text{\AA}$ ), indicative of the  $\alpha$  agostic interaction.

Since the vacant  $d_{xz}$  orbital is believed to play a critical role in the agostic interaction, we employed the BLW method to re-optimize both the  $C_s$  and  $C_{2v}$  geometries by constraining the  $d_{xz}$  orbital to be strictly vacant. Surprisingly, both converge to the same geometry. In other words, the agostic structure of  $C_s$  symmetry would resume to a usual metal alkylidene structure of  $C_{2v}$  symmetry if the  $d_{xz}$  orbital were removed from any interaction with occupied orbitals. As a consequence, the adiabatic delocalization energy (ADE), which measures the energy difference between the optimal DFT and the optimal BLW computations, is 7.3 kcal/mol and 5.8 kcal/mol for  $C_s$  and  $C_{2v}$  symmetries respectively. However, the vertical delocalization energy (VDE, energy difference between DFT and BLW states at the same DFT optimal geometry) dramatically reaches up to 24.5 kcal/mol for agostic  $C_s$  structure, indicating that the significant agostic interaction (24.5 kcal/mol) is largely biased or offset by the structural deformation cost ( $24.5 - 7.3 = 17.2$  kcal/mol). In other words, the seemingly marginal agostic effect (1.5 kcal/mol) from the non-agostic  $C_{2v}$  structure to the agostic  $C_s$  structure results from a strong and stabilizing orbital interactions and similarly strong but destabilizing deformation penalty.

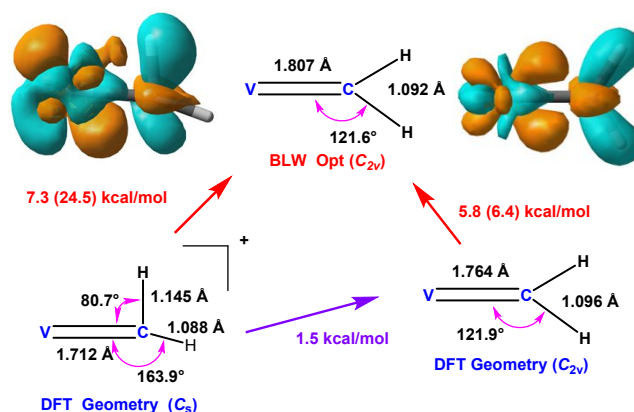


**Figure 3.** Key structural parameters for  $[\text{VCH}_2]^+$  optimized by the regular DFT and BLW methods at the  $C_s$  and  $C_{2v}$  symmetries. The data on the arrows represent the ADEs, while the data in brackets refer to the VDEs. The EDD maps (at the isovalues of 0.003 a.u. for  $C_s$ , left, and 0.001 a.u. for  $C_{2v}$ , right) show the electron movement toward the  $d_{xz}$  orbital, where the orange and cyan colors refer to the gain and loss of the electron density, respectively.

To seek an improved understanding of the bonding nature of  $[\text{V}=\text{CH}_2]^+$ , we break it into two fragments,  $\text{V}^+$  and carbene (singlet), and track the energy evolution of orbitals from isolated carbene monomer, deformed carbene monomers in  $C_{2v}$  and  $C_s$  symmetries in the existence of  $\text{V}^+$  which exerts an electric field, and to the final compound. The shifting of energy levels of frontier molecular orbitals in various monomers are quite minor

and negligible. However, the  $\pi_{\text{CH}_2}$  orbital pivots from the  $C_{2v}$  structure to the  $C_s$  structure, making itself more compatible to interact effectively with the  $d_{xz}$  orbital. As seen from Fig. 4, the  $\pi_{\text{CH}_2}$  orbital interacts with the  $d_{xz}$  orbital rather than the distortive  $\sigma$  lone pair orbital.

It should be noted that both  $C_s$  and  $C_{2v}$  geometries exhibit the similar distributions of canonical MOs, which interact with  $V^+$  differently due to the different orientations (leading the different orbital overlaps). This can be reflected from the very different vertical delocalization energies 24.5 kcal/mol and 6.4 kcal/mol for the  $C_s$  and  $C_{2v}$  geometries, respectively, and the electron density difference (EDD) maps between DFT and BLW states (Fig. 3). Therefore, the metal-carbon bond in  $[V=\text{CH}_2]^+$  should be best defined as a partial triple bond, in which the third bond refers to the  $\pi_{\text{CH}_2} \rightarrow d_{xz}$  orbital interaction, or the true origin of agostic interaction.

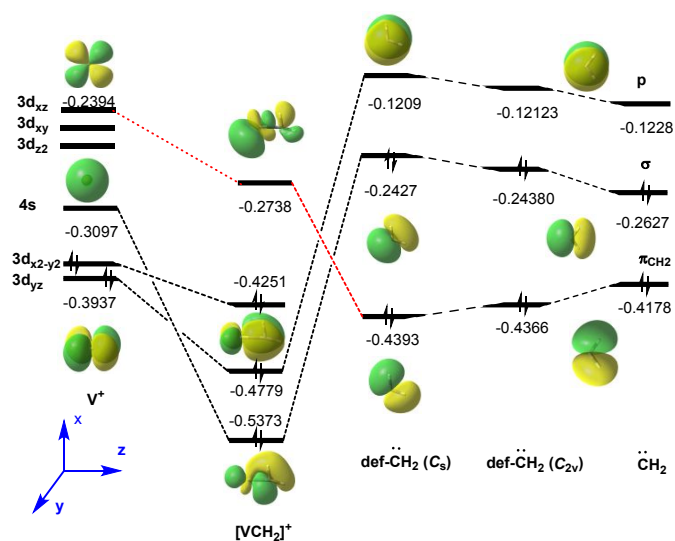


**Figure 4.** Orbital correlation diagram for the complex of  $\text{CH}_2$  and  $V^+$ , in which def- refers to deformed (but isolated) geometries. Energies are at the atomic units.

In order to validate this partial triple bonding model in general TM carbenes, we continue to study chloride-bonded  $[\text{Cl}_2\text{VCHMe}]^-$  and  $[\text{Cl}_2\text{VCHMe}]^+$  systems. It has been recognized that cationic TM compounds usually display more significant agostic characters than neutral and even anionic counterparts. However, here we found that anionic  $[\text{Cl}_2\text{VCHMe}]^-$  is much more agostic than cationic  $[\text{Cl}_2\text{VCHMe}]^+$ , though the latter is more electrophilic than the former (Fig. 5).

There are two major differences between these anionic and cationic systems. One lies in the electronic configurations, in which  $[\text{Cl}_2\text{VCHMe}]^-$  represents typical Fischer-type TM carbene consisting of two dative bonds,<sup>6, 31</sup> while  $[\text{Cl}_2\text{VCHMe}]^+$  is a Schrock-type carbene<sup>32, 33</sup> with two electron-sharing bonds (the triplets of  $[\text{VCl}_2]^+$  and  $\text{CHMe}$  are more stable than their singlet counterparts by 27.3 kcal/mol and 59.6 kcal/mol respectively). However, this is not the cause why  $[\text{Cl}_2\text{VCHMe}]^-$  is more agostic than  $[\text{Cl}_2\text{VCHMe}]^+$ , as they both possess an vacant  $d_{xz}$  orbital to accept the electron density from the  $\pi_{\text{CHMe}}$  orbital. The more decisive difference is the orientation of the two chloride ligands. The two chlorides are nearly perpendicular to the  $d_{xz}$  plane in

$[\text{Cl}_2\text{VCHMe}]^-$ , but they are in the same plane with the  $d_{xz}$  orbital in  $[\text{Cl}_2\text{VCHMe}]^+$ . As a consequence, the  $\pi_{\text{CHMe}} \rightarrow d_{xz}$  interaction in  $[\text{Cl}_2\text{VCHMe}]^-$  is much stronger than that in  $[\text{Cl}_2\text{VCHMe}]^+$ . Specifically, chloride ligands have little interference with the  $\pi_{\text{CHMe}} \rightarrow d_{xz}$  interaction in  $[\text{Cl}_2\text{TiCHMe}]^-$ , which thus is essentially comparable to  $[\text{V}=\text{CH}_2]^+$  and exhibits significant agostic characters. In sharp contrast, in  $[\text{Cl}_2\text{VCHMe}]^+$ , the  $d_{xz}$  orbital tends to accept electron density from chlorines rather than the  $\pi_{\text{CHMe}}$  orbital, leading to the impairment of the agostic interaction.

The BLW method can be used to further clarify the role of  $\pi \rightarrow d_{xz}$  interaction in the  $\alpha$ -agostic effect by keeping the  $d_{xz}$  orbital vacant. It is obvious that both BLW optimal structures exhibit few agostic characters any more. Notably, the ADE in  $[\text{Cl}_2\text{VCHMe}]^+$  with insignificant agostic effect reaches to 37.5 kcal/mol, while it is only 14.6 kcal/mol in the agostic  $[\text{Cl}_2\text{VCHMe}]^-$ . As discussed above,  $\pi_{\text{CHMe}} \rightarrow d_{xz}$  bonding is prominent in  $[\text{Cl}_2\text{VCHMe}]^-$  and thus nearly all 14.6 kcal/mol can be ascribed to the agostic interaction. As for  $[\text{Cl}_2\text{VCHMe}]^+$ , the 37.5 kcal/mol mainly comes from the  $\pi_{\text{Cl}_2} \rightarrow d_{xz}$  interaction supplemented with secondary  $\pi_{\text{CHMe}} \rightarrow d_{xz}$ , as chloride atom is a much stronger  $\pi$  electron-donating group than  $\text{CHMe}$  group. These conclusions can be endorsed by the electron movements to the  $d_{xz}$  orbital as revealed by EDD maps. As shown in Fig. 5, it is obvious that the  $d_{xz}$  orbital would not interact with regular or distortive lone pair of the carbene fragment (as proposed in Goddard's bonding model), yet accept electron density from occupied orbital of appropriate symmetry in ligands, i.e., chlorine atoms or  $\pi_{\text{CHMe}}$  orbital in the carbene fragment.

From the pretext, one can see that the ancillary ligands are able to affect the strength of the  $\pi_{\text{CHR}} \rightarrow d_{xz}$  bonding and thus modulate the agostic effect. To this end, we used  $[\text{R}'\text{Cl}_2\text{VCHMe}]$  ( $\text{R}' = \text{CH}_2\text{CH}_3, \text{Cl}, \text{C}_5\text{H}_5, \text{OCH}_3, \text{CN}$  and  $\text{CO}$ ) to demonstrate the modulation mechanism of ancillary ligands on the  $\alpha$ -agostic interaction.

As the reference for subsequent comparisons, we first studied the system  $[\text{CH}_3\text{CH}_2\text{Cl}_2\text{VCHMe}]$ , where the ethyl ligand is neither a  $\pi$  electron donating group ( $\pi$ -EDG) nor a  $\pi$  electron withdrawing group ( $\pi$ -EWG). As a consequence, it exhibits comparable agostic interaction with respect to  $[\text{VCH}_2]^+$  and  $[\text{Cl}_2\text{VCHMe}]^-$ . In sharp contrast, when  $\text{R}'$  is replaced by  $\pi$ -EDGs such as  $\text{Cl}, \text{OCH}_3$  and  $\text{C}_5\text{H}_5$ , the agostic interaction becomes weaker than that in  $[\text{CH}_3\text{CH}_2\text{Cl}_2\text{VCHMe}]$ , as demonstrated by enlarged  $\text{V}-\text{C}-\text{H}$  angles and shortened  $\text{C}-\text{H}$  bond distances. It has been shown previously that  $\pi \rightarrow d_{xz}$  interaction has two origins, one coming from  $\pi_{\text{R}'} \rightarrow d_{xz}$ , and the other being concerning  $\pi_{\text{CHMe}} \rightarrow d_{xz}$ . Only the latter is responsible for the agostic effect. The strength of the overall  $\pi \rightarrow d_{xz}$  interaction is thus obviously dependent on the capacity of the  $d_{xz}$  orbital as well as the  $\pi$  electron donating abilities of ligands. Therefore,  $\pi$ -EDGs substituted  $[\text{R}'\text{Cl}_2\text{VCHMe}]$  exhibit nearly identical ADEs (34.2, 38.2, 35.6 kcal/mol for  $\text{Cl}, \text{C}_5\text{H}_5$  and  $\text{OCH}_3$  respectively). In contrast, more agostic complex  $[\text{CH}_3\text{CH}_2\text{Cl}_2\text{VCHMe}]$  results in a smaller ADE with 25.2 kcal/mol. This can be ascribed to the weakened  $\pi_{\text{R}'} \rightarrow d_{xz}$  interaction in  $[\text{CH}_3\text{CH}_2\text{Cl}_2\text{VCHMe}]$  though the agostic  $\pi_{\text{CHMe}} \rightarrow d_{xz}$  interaction gets much stronger. According to this assumption,  $\pi$ -EWGs are expected to impair the  $\pi_{\text{R}'} \rightarrow d_{xz}$

interaction and thus enhance the  $\pi_{\text{CHMe}} \rightarrow d_{xz}$  interaction. However,  $\pi$ -EWGs such as CN and NO would not lead to stronger agostic interaction than  $[\text{CH}_2\text{CH}_3\text{Cl}_2\text{VCHMe}]$ . This is because

**Table 1.** Optimal bond distances (Å), angles (degree), vibrational frequencies of the CH' group ( $\nu$  in  $\text{cm}^{-1}$ ) and the  $\pi \rightarrow d_{xz}$  charge transfer energies ( $\Delta E$ , in kcal/mol) at the PBE0-D3 level for  $[\text{R}'\text{Cl}_2\text{VCHMe}]$ .

R'	Method	$\vartheta_{\text{MCH}}$	$\vartheta_{\text{MCC}}$	$R_{\text{M-C}}$	$R_{\text{M-H}}$	$R_{\text{C-H}}$	$\nu_{\text{CH}'}$	$\Delta E$
CH <sub>2</sub> CH <sub>3</sub>	DFT	77.7	164.9	1.715	1.847	1.144	2683	25.2
	BLW	113.2	130.1	1.814	2.460	1.094	3121	
Cl	DFT	89.9	150.4	1.730	2.057	1.117	2915	34.2
	BLW	111.1	130.4	1.800	2.419	1.093	3128	
C <sub>5</sub> H <sub>5</sub>	DFT	88.1	155.4	1.755	2.049	1.116	2914	38.2
	BLW	99.1	146.3	1.807	2.259	1.099	3071	
OCH <sub>3</sub>	DFT	100.8	140.9	1.754	2.242	1.105	3014	35.6
	BLW	116.1	125.0	1.808	2.489	1.092	3154	
CN	DFT	99.5	141.7	1.750	2.219	1.107	3006	32.3
	BLW	115.5	124.0	1.790	2.465	1.091	3162	
CO	DFT	105.3	138.0	1.792	2.341	1.106	3013	45.3
	BLW	116.2	122.7	1.816	2.498	1.092	3162	

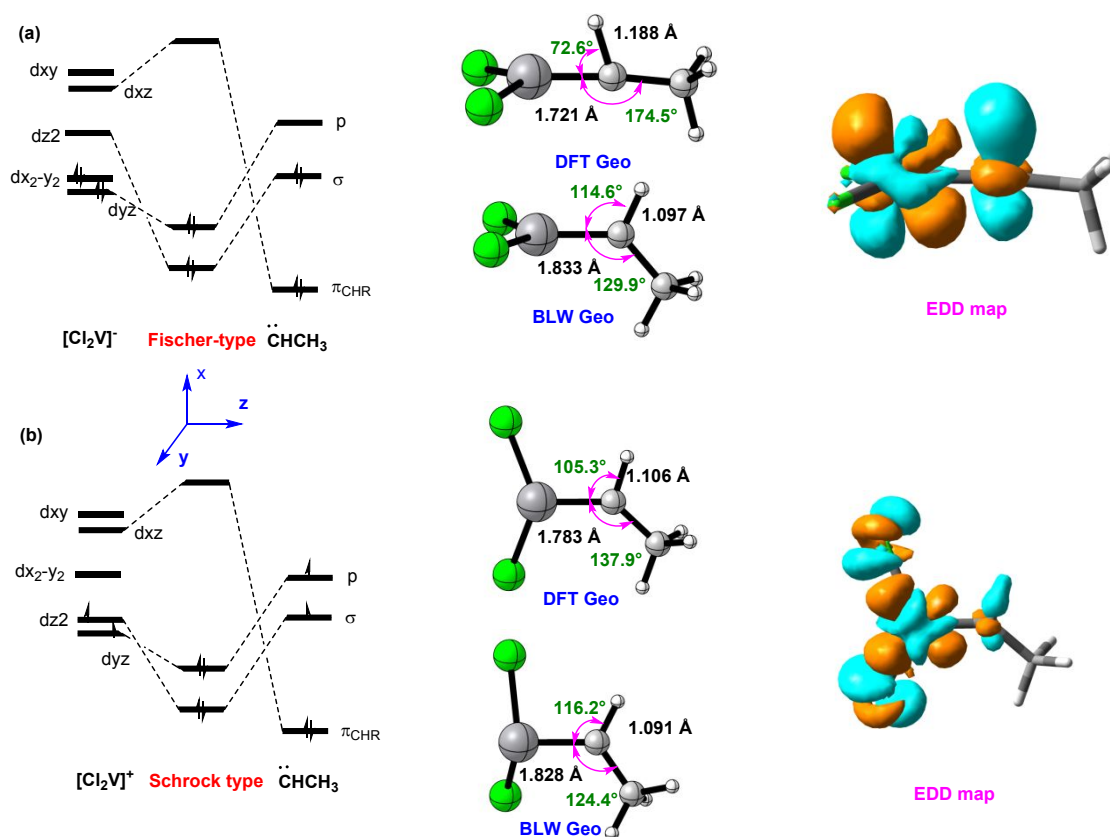


**Figure 5.** Orbital interaction diagrams and optimized DFT and BLW structures for (a)  $[\text{Cl}_2\text{VCHMe}]^-$  and (b)  $[\text{Cl}_2\text{VCHMe}]^+$  and their EDD maps (isovalue = 0.003 au).

$\pi$ -EWGs change the orientations of ligands (see Fig. 6), which is quite from the the  $\pi$  EDGs or ethyl substituted  $[\text{R}'\text{Cl}_2\text{VCHMe}]$  but similar to the  $[\text{Cl}_2\text{VCHMe}]^+$ . As a consequence, the  $\pi_{\text{CHMe}} \rightarrow d_{xz}$  and  $\pi_{\text{Cl}} \rightarrow d_{xz}$  (not  $d_{xz} \rightarrow \pi_{\text{CO/CN}}$ ) interactions would compete for providing the electron density to the metal center and thus lead to moderate agostic structures.

Apart from the electronic effect, steric hindrance of large ligands also plays an important role in agostic interactions. By comparing the BLW optimal geometries between  $[\text{CpCl}_2\text{VCHMe}]$  and  $[\text{Cl}_3\text{VCHMe}]$ , it is clear that  $[\text{CpCl}_2\text{VCHMe}]$  also exhibits a moderate agostic structure, which is even comparable to the DFT optimal geometry of  $[\text{OCH}_3\text{Cl}_2\text{VCHMe}]$ .

This unusual phenomenon can be ascribed to the steric hindrance of larger Cp ligands, which inhibit the rotation of M-C-

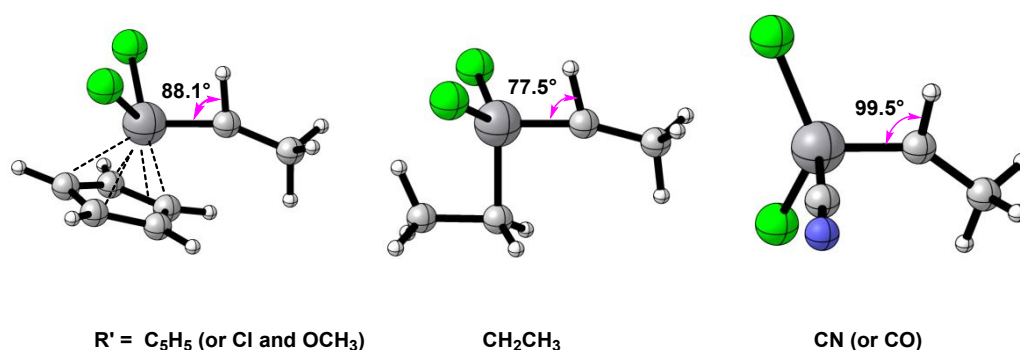


**Figure 6.** Optimal DFT geometries for  $[\text{R}'\text{Cl}_2\text{VCHMe}]$  ( $\text{R}' = \text{C}_5\text{H}_5, \text{CH}_2\text{CH}_3, \text{CN}$ )

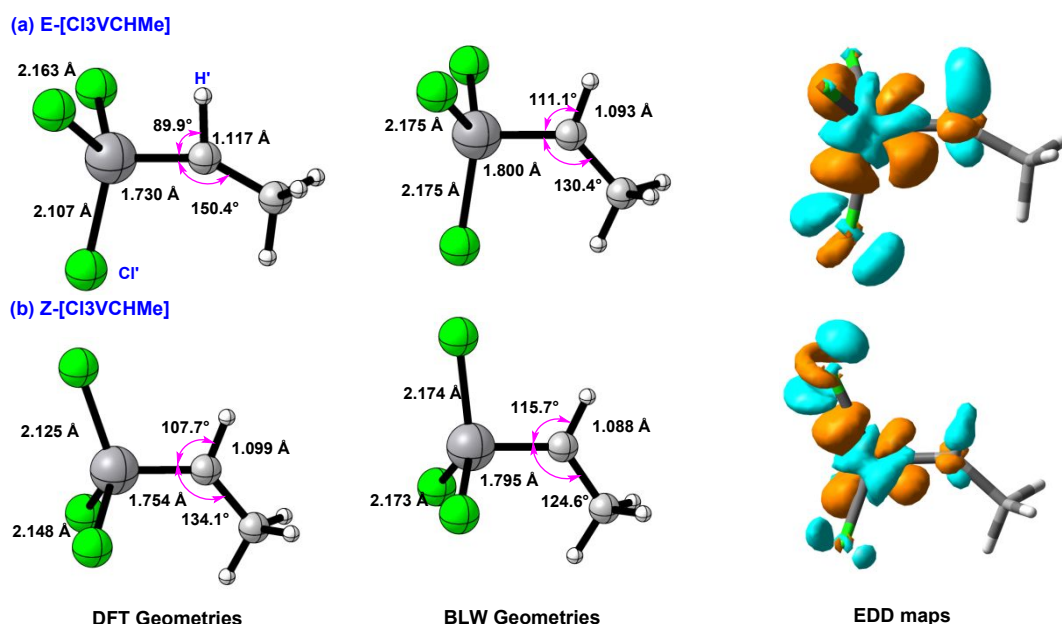


**Figure 7.** Optimal DFT, BLW geometries and EDD maps (isovalue = 0.003 au) for two stereoisomers of  $[\text{Cl}_3\text{VCHMe}]$ .

Notably, we found that  $[\text{Cl}_3\text{VCHMe}]$  has two stereoisomers, which are noted as Z- $[\text{Cl}_3\text{VCHMe}]$  and E- $[\text{Cl}_3\text{VCHMe}]$  for comparison. Specially, in Z- $[\text{Cl}_3\text{VCHMe}]$ , both H' and Cl' atoms are placed in the same side, while they lie in the opposite side in E- $[\text{Cl}_3\text{VCHMe}]$ . Their absolute energies are nearly identical (agostic E- $[\text{Cl}_3\text{VCHMe}]$  is only a little more stable than Z- $[\text{Cl}_3\text{VCHMe}]$  by 0.1 kcal/mol). It seems that the orientation of ligands in E- $[\text{Cl}_3\text{VCHMe}]$  also plays an important role in the formation of agostic interaction, which leaves the space for the C–H bond to bend towards the metal centre. When the  $\pi \rightarrow d_{xz}$  interaction was “shut down” by the BLW method, both the BLW optimal geometries behave as usual TM alkylidene structures, and the ADEs in E- $[\text{Cl}_3\text{VCHMe}]$  (34.2 kcal/mol) is only slightly higher than that in Z- $[\text{Cl}_3\text{VCHMe}]$  (31.5 kcal/mol). It should be stressed here that the ADEs are also comparable to that in  $[\text{Cl}_2\text{VCHMe}]^+$ , because they have similar  $\pi \rightarrow d_{xz}$  charge transfer interaction. However, the  $\pi_{\text{CHMe}} \rightarrow d_{xz}$

interaction in E- $[\text{Cl}_3\text{VCHMe}]$  is more significant than that in Z- $[\text{Cl}_3\text{VCHMe}]$ , which is also evidenced by the EDD maps in Fig. 7.

Summarizing the above analyses, we conclude that the ancillary ligands can modulate the agostic interaction through electronic and steric effects. In particular, it can not only compete with the carbene fragment for the interaction with the metal center, but also alters the orientation of ligands towards the metal center.

The  $\alpha$ -agostic interaction have been observed experimentally in a set of well-defined silica-supported alkylidene metal compounds ( $\equiv\text{SiO})(\text{X})\text{M}(\text{R}')(\text{=CHtBu})$  involving third row metals.<sup>34–36</sup> These compounds share the same alkylidene framework and differ by metal centers and ancillary ligands, with  $\text{M}(\text{R}') = \text{TaCH}_2\text{tBu}$ ,  $\text{WNAr}$  or  $\text{ReCtBu}$  and X = alkyl or pyrrolyl. Our computed parameters typically the M–C–H angles are well consistent with literatures as shown in Fig. 8. Here, we applied the same theoretical scheme to study their simplified model

systems, noted as 4-Ta, 5-W and 6-Re. It can be seen from Fig. 8 that the agostic interaction is strongly present in 4-Ta but moderate in 5-W and 6-Re. This can be ascribed to the  $\pi$  electron donating nature of ancillary ligands. The strong  $\pi$ -EDGs  $\equiv\text{CMe}$  and  $=\text{NPh}$  in 5-W and 6-Re dramatically enhance the  $\pi_{\text{R}'} \rightarrow d_{xz}$  and impair the agostic  $\pi_{\text{CHMe}} \rightarrow d_{xz}$  bonding, and the ADEs between DFT and BLW states are measured by 68.2 kcal/mol and 105.7 kcal/mol respectively, which is much larger than that in 4-Ta (28.3 kcal/mol). However, the ADE in 4-Ta mainly originates from the  $\pi_{\text{CHMe}} \rightarrow d_{xz}$  interaction, leading to the strongest agostic interaction among the three model systems. Nevertheless, all BLW optimal geometries without the  $\pi \rightarrow d_{xz}$  interaction result in usual alkylidene structures with negligible agostic interaction.

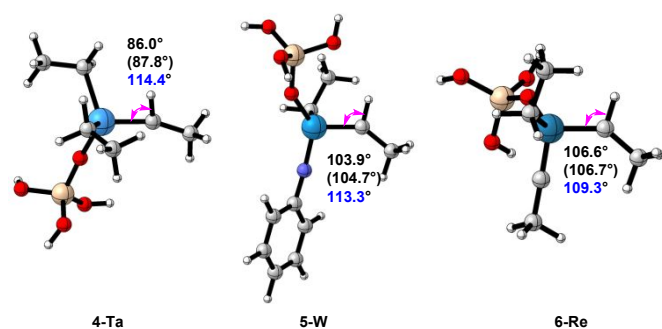


**Figure 8.** Optimal DFT geometries for computational models of well-known experimental metal alkylidene compounds, in which the black and blue data represent M–C–H angles from DFT and BLW optimizations respectively, the angles in brackets are from Ref. 34.

## Conclusions

In conclusion, the present theoretical calculations provide direct evidence for the existence of a three-center two-electron  $\pi_{\text{CHR}} \rightarrow d_{\text{M}}$  bonding and its dominant role on the formation of  $\alpha$ -agostic interaction in exemplary TM carbene compounds. Accordingly, the metal-carbon bonds in agostic TM carbenes can be best defined as a partial triple bonding, consisting of well-defined  $\sigma$  and  $\pi$  bonds as well as a weak yet decisive  $\pi_{\text{CHR}} \rightarrow d_{\text{M}}$  interaction. In addition, the electronic and steric effects of ancillary ligands have been proved to be able to modulate the agostic interaction.

## Experimental Section

All DFT and BLW geometry optimizations and frequency calculations were performed with the GAMESS software<sup>37</sup> at the PBE0 level<sup>38</sup> augmented by Grimme's D3 dispersion correction<sup>39, 40</sup>, and the optimal structures are visualized through CYLview software<sup>41</sup>. The relativistic core potential (RECP) from the Stuttgart group and the associated basis set<sup>42-44</sup> were adopted for all transition metals, while the remaining main-group atoms (H, C, N, O, Cl and Si) were represented by 6-311G(d,p) basis set. Details on the BLW method can be found in the Supporting Information.

## Author Contributions

XL, WW and YM conceived the project, XL and WT performed the research, XL and YM wrote the manuscript.

## Conflicts of interest

There are no conflicts to declare.

## Acknowledgements

This project is supported by the National Natural Science Foundation of China (Nos. 22103064, 21733008 and 21973077) and the Opening Project of PCOSS, Xiamen University (No. 202119). This work was performed in part at the Joint School of Nano-science and Nanoengineering, a member of the Southeastern Nanotechnology Infrastructure Corridor (SENIC) and National Nanotechnology Coordinated Infrastructure (NNCI), which is supported by the National Science Foundation (Grant ECCS-2025462).

## References

1. R. R. Schrock, *Angew. Chem. Int. Ed.*, 2006, **45**, 3748-3759.
2. J.-M. Basset, C. Coperet, D. Soulivong, M. Taoufik and J. T. Cazat, *Acc. Chem. Res.*, 2010, **43**, 323-334.
3. H. M. L. Davies and J. S. Alford, *Chem. Soc. Rev.*, 2014, **43**, 5151-5162.
4. C. Coperet, *Chem. Rev.*, 2010, **110**, 656-680.
5. Y. Chen, E. Abou-hamad, A. Hamieh, B. Hamzaoui, L. Emsley and J.-M. Basset, *J. Am. Chem. Soc.*, 2015, **137**, 588-591.
6. E. O. Fischer and A. Maasböl, *Angew. Chem. Int. Ed.*, 1964, **3**, 580-581.
7. G. Frenking and N. Froehlich, *Chem. Rev.*, 2000, **100**, 717-774.
8. A. Krapp, K. K. Pandey and G. Frenking, *J. Am. Chem. Soc.*, 2007, **129**, 7596-7610.
9. D. Benitez, N. D. Shapiro, E. Tkatchouk, Y. Wang, W. A. Goddard and F. D. Toste, *Nat. Chem.*, 2009, **1**, 482-486.
10. K. Yamamoto, C. P. Gordon, W.-C. Liao, C. Copéret, C. Raynaud and O. Eisenstein, *Angew. Chem. Int. Ed.*, 2017, **56**, 10127-10131.
11. R. J. Goddard, R. Hoffmann and E. D. Jemmis, *J. Am. Chem. Soc.*, 1980, **102**, 7667-7676.
12. M. Brookhart, M. L. H. Green and M. L. H., *J. Organomet. Chem.*, 1983, **250**, 395-408.
13. M. Brookhart, M. L. H. Green and L. L. Wong, *Prog. Inorg. Chem.*, 1988, **36**, 1-124.
14. M. Brookhart, M. L. H. Green and G. Parkin, *Proc. Natl. Acad. Sci.*, 2007, **104**, 6908.
15. W. Scherer and G. S. McGrady, *Angew. Chem. Int. Ed.*, 2004, **43**, 1782-1806.
16. C. P. Gordon, D. B. Culver, M. P. Conley, O. Eisenstein, R. A. Andersen and C. Copéret, *J. Am. Chem. Soc.*, 2019, **141**, 648-656.
17. X. Lin and Y. Mo, *Inorg. Chem.*, 2022, **61**, 2892-2902.
18. O. Eisenstein and Y. Jean, *J. Am. Chem. Soc.*, 1985, **107**, 1177-1186.

19. A. Haaland, W. Scherer, K. Ruud, G. S. McGrady, A. J. Downs and O. Swang, *J. Am. Chem. Soc.*, 1998, **120**, 3762-3772.
20. Q. Lu, F. Neese and G. Bistoni, *Angew. Chem. Int. Ed.*, 2018, **57**, 4760-4764.
21. X. Lin, W. Wu and Y. Mo, *Coord. Chem. Rev.*, 2020, **419**, 213401.
22. C. P. Gordon, K. Yamamoto, K. Searles, S. Shirase, R. A. Andersen, O. Eisenstein and C. Copéret, *Chem. Sci.*, 2018, **9**, 1912-1918.
23. D. Cooper, *Valence bond theory*, Elsevier, 2002.
24. S. S. Shaik and P. C. Hiberty, *A chemist's guide to valence bond theory*, John Wiley & Sons, 2007.
25. W. Wu, P. Su, S. Shaik and P. C. Hiberty, *Chem. Rev.*, 2011, **111**, 7557-7593.
26. L. Pauling, *The Nature of the Chemical Bond*, Cornell university press Ithaca, NY, 1960.
27. Y. Mo and S. D. Peyerimhoff, *J. Chem. Phys.*, 1998, **109**, 1687-1697.
28. Y. Mo, L. Song and Y. Lin, *The Journal of Physical Chemistry A*, 2007, **111**, 8291-8301.
29. Y. Mo, in *The Chemical Bond: Fundamental Aspects of Chemical Bonding* *The Chemical Bond*, eds. G. Frenking and S. Shaik, 2014, DOI: <https://doi.org/10.1002/9783527664696.ch6>, ch. 6, pp. 199-232.
30. I. Vidal, S. Melchor and J. A. Dobado, *The Journal of Physical Chemistry A*, 2005, **109**, 7500-7508.
31. E. O. Fischer, G. Kreis, C. G. Kreiter, J. Müller, G. Huttner and H. Lorenz, *Angew. Chem. Int. Ed.*, 1973, **12**, 564-565.
32. R. R. Schrock, *J. Am. Chem. Soc.*, 1974, **96**, 6796-6797.
33. S. J. McLain, C. D. Wood, L. W. Messerle, R. R. Schrock, F. J. Hollander, W. J. Youngs and M. R. Churchill, *J. Am. Chem. Soc.*, 1978, **100**, 5962-5964.
34. S. Halbert, C. Copéret, C. Raynaud and O. Eisenstein, *J. Am. Chem. Soc.*, 2016, **138**, 2261-2272.
35. F. Blanc, J.-M. Basset, C. Copéret, A. Sinha, Z. J. Tonzetich, R. R. Schrock, X. Solans-Monfort, E. Clot, O. Eisenstein, A. Lesage and L. Emsley, *J. Am. Chem. Soc.*, 2008, **130**, 5886-5900.
36. K. W. Chan, D. Mance, O. V. Safonova and C. Copéret, *J. Am. Chem. Soc.*, 2019, **141**, 18286-18292.
37. M. W. Schmidt, K. K. Baldrige, J. A. Boatz, S. T. Elbert, M. S. Gordon, J. H. Jensen, S. Koseki, N. Matsunaga, K. A. Nguyen, S. Su, T. L. Windus, M. Dupuis and J. A. Montgomery Jr, *J. Comput. Chem.*, 1993, **14**, 1347-1363.
38. C. Adamo and V. Barone, *J. Chem. Phys.*, 1999, **110**, 6158-6170.
39. S. Grimme, J. Antony, S. Ehrlich and H. Krieg, *J. Chem. Phys.*, 2010, **132**, 154104.
40. S. Grimme, S. Ehrlich and L. Goerigk, *J. Comput. Chem.*, 2011, **32**, 1456-1465.
41. *Journal*.
42. M. Dolg, U. Wedig, H. Stoll and H. Preuss, *J. Chem. Phys.*, 1987, **86**, 866-872.
43. D. Andrae, U. Häußermann, M. Dolg, H. Stoll and H. Preuß, *Theor. Chim. Acta*, 1990, **77**, 123-141.
44. J. M. L. Martin and A. Sundermann, *J. Chem. Phys.*, 2001, **114**, 3408-3420.